Study on the Dimensionality of Flux Dynamics in Superconducting YBCO/PYBCO Superlattices

S. Y. Yang[1], J. T. Jeng[1], H. E. Horng[1], and H. C. Yang[2]

[1]*Department of Physics, National Taiwan Normal University, Taipei, Taiwan 117, R.O.C.*
[2]*Department of Physics, National Taiwan University, Taipei, Taiwan 106, R.O.C.*

(Received December 20, 1997)

Angular dependent critical current densities for superconducting $YBa_2Cu_3O_{7-y}$/$Pr_{0.5}Y_{0.5}Ba_2Cu_3O_{7-y}$ superlattices and a pure $YBa_2Cu_3O_{7-y}$ thin film were measured to investigate the influence of temperature, thickness of each $YBa_2Cu_3O_{7-y}$ layer and the applied magnetic filed on the dimensionality of flux dynamics (DFD). It was found that the DFD in the superlattice (48Å/24Å) x20 exhibits a 2D behavior at $t = 0.65$, but that it deviates from the 2D behavior as $t = 0.92$. By increasing the thickness of each $YBa_2Cu_3O_{7-y}$ layer from 48Å to 120Å, the DFD becomes closer to 2D at $t = 0.92$ under H = 0.1 T. The DFD in the superlattice (120Å/24Å) x8 exhibits a 2D behavior at $t = 0.92$ if the ab-plane component of applied magnetic field H^{ab} is smaller than 1 T, but it deviates from 2D if H^{ab} is larger than 1 T. The flux mechanics are discussed.

PACS. 74.90.+n – Other topics in superconductivity.
PACS. 74.80.Dm – Superconducting layer structures: superlattices, heterojunctions, and multilayers

I. Introduction

The dimensionality of flux dynamics for high-T, superconductors attracts much attention. Taking into account the layered structure of high-T, superconductors, Tachiki et al. proposed an anisotropic 3D model in which the weakly superconducting layers act as strong and intrinsic pinning centers for the string vortices, as shown in Fig. 1 [1]. The weak and extrinsic pinning centers for pancake vortices may be the point defects, impurities or twin boundaries [2]. Some experimental results of angular dependent critical current densities $J_c(\theta)$ for $YBa_2Cu_3O_{7-y}$ thin films can be fitted to this anisotropic 3D model very well [3,4]. On the other hand, because the c-axis Ginzburg-Landau coherence length ξ_c is smaller than the c-axis lattice constant except at the temperatures near T_c in high-T, superconductors, the order parameter between CuO_2 planes is almost zero. Thus, Kes *et al.* predicted that the critical current density $J_c(H,\theta)$ is determined by the c-axis component of the applied magnetic field and pointed out that $J_c(H,\theta)$ should follow the 2D scaling law: $J_c(H,\theta) = J_c(H\cos\theta, 0°)$, here θ is the angle between the c axis of the sample and the applied magnetic field [5]. Further, Clem proposed a 2D pancake vortex model [6]. According to this model, the magnetic field parallel to the CuO_2 plane (ab planes) can penetrate completely and dissipation results from the motion of pancake vortices. Some experimental results for $J_c(\theta)$ in $YBa_2Cu_3O_{7-y}$ superconducting superlattices can be fitted to this 2D model very well [7,8].

© 1998 THE PHYSICAL SOCIETY OF THE REPUBLIC OF CHINA

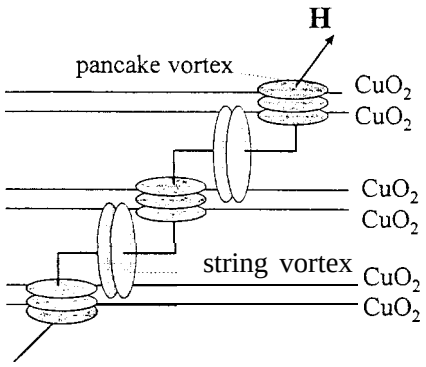


FIG. 1. Geometry of string and pancake vortices. The string vortices are pinned at weakly superconducting layers and the pancake vortices exist in the CuO_2 planes (ate planes).

A number of experiments revealed that the dimensionality of flux dynamics in $YBa_2Cu_3O_{7-y}$ thin films and superlattices is affected by many factors [9-11]. In this work, the influences of temperature, the thickness of each $YBa_2Cu_3O_{7-y}$ layer and of applied magnetic field on the dimensionality of flux dynamics in various $YBa_2Cu_3O_{7-y}/Pr_{0.5}Y_{0.5}Ba_2Cu_3O_{7-y}$ superlattices was investigated by measuring the critical current density $J_c(\theta)$.

II. Experimental details

$YBa_2Cu_3O_{7-y}/Pr_{0.5}Y_{0.5}Ba_2Cu_3O_{7-y}$ (YBCO/PYBCO) superlattices (denoted by sample A, B and C) and a YBCO (refered to as sample D) thin film were deposited onto $SrTiO_3(001)$ substrates. The deposition and patterning methods for all samples was reported in our previous study [10]. The thickness of each YBCO layer in the superlattices varied from 48 Å to 120 Å, but the total thickness of the YBCO layers was kept at 960 A. The configurations and critical temperatures $T_{c,zero}$ of the samples are listed in Table I. The powder x-ray diffracton patterns for samples A, B and C were probed to confirm superlattice structures. In order to measure the angular dependent critical current, each sample was mounted on a rotatable sample holder with a resolution of 0.01" for the angle θ spanned by the c axis of the sample and the applied magnetic field **H.** The field is provided by a superconducting magnet with range between 10 Gauss and 7 T. The cooling system is OXFORD SM-7 and the temperature can vary from 1.5 K to 300 K. The four-probe method is used for measuring the critical current density J_c and the criterion voltage for J_c is **5** $\mu V/mm$. The current was applied along the rotating axis (y axis) shown in Fig. 2. Thus, the ab-plane and the c-axis components of the Lorentz force (denoted by $F_{L,ab}$ and $F_{L,c}$) are $(1/c)JH\cos\theta$ and $(1/c)JH\sin\theta$, respectively. These two forces cause the pancake vortices and string vortices to move. Hence, by comparing the experimental value of $J_c(\theta)$ to the 2D scaling law, one can examine the dimensionality of flux dynamics.

TABLE I. Film configurations and $T_{c,zero}$ for the YBCO/PYBCO superlattices and the pure YBCO thin film. Each superlattice has a total 960 A-thick $YBa_2Cu_3O_{7-y}$ layers.

Sample no.	A	B	C	D
Sample Configuration	YBCO/PYBCO (48Å/24Å) x20	YBCO/PYBCO (60Å/24Å) x 16	YBCO/PYBCO (120Å/24Å)×8	YBCO 960Å
$T_{c,zero}$(K)	76.5	78.5	80.2	87.5

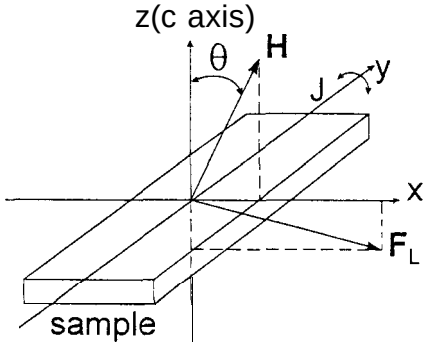


FIG. 2. Configuration of the applied current density J, applied magnetic field **H** and Lorentz force F_L.

III. Results and discussion

The powder x-ray diffraction patterns are shown in Fig. 3. The satellite peaks beside the YBCO(001) peak were found clearly and the modulation wavelengthes A were 72 A, 84 Å and 144 Å for samples A, B and C respectively. These results imply the good sample quality.

The angular dependent critical current densities $J_c(\theta)$ for sample A were measured at the reduced temperature $t \equiv T/T_{c,zero} = 0.65$ and 0.92. The $J_c(\theta)$ curves at $t = 0.65$ under applied fields $H \leq 5$ T are shown in Fig. 4 and are fitted to the 2D scaling law represented by the solid lines. It was found that all the $J_c(\theta)$ curves can be fitted to the scaling law very well. The $J_c(\theta)$ curves at $t = 0.92$ for $H \leq 1$ T are plotted in Fig. 5 and are compared with the scaling law denoted by solid lines. These curves deviate from the scaling law, so that the dimensionality of flux dynamics in sample A exhibits a 2D behavior at $t = 0.65$ for $H \leq 5$ T, but deviates from this 2D behavior as t is increased to 0.92 and the string vortices contribute to the energy dissipation.

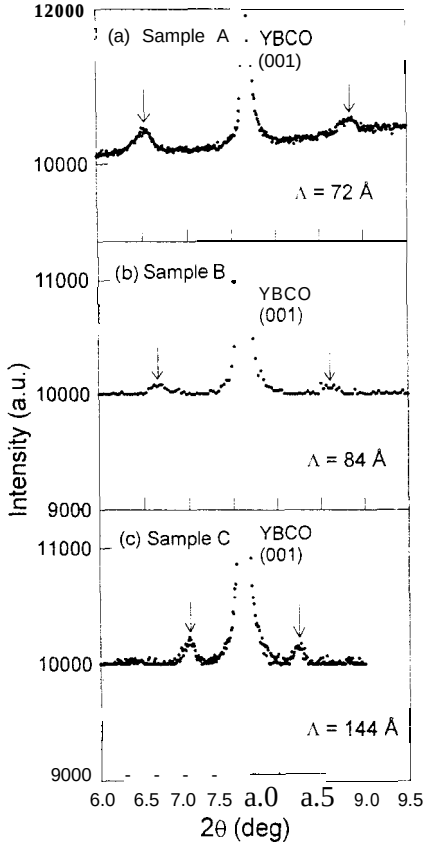


FIG. 3. Powder x-ray diffraction patterns for superlattices. Note the satellite peaks. The modulation wavelengthes A were 72 Å, 84 Å and 144 Å for samples A, B and C respectively.

Our previous study indicated that the occurrence of string vortices at higher temperatures is not related to the PYBCO layer but can be explained in terms of the temperature dependent c-axis GL coherence length ξ_c in YBCO layers [12]. At the lower temperature, $\xi_c(t = 0.65)$ is about 5 Å according to the approximation $\xi_c(0)/(1\text{-}t)^{1/2}$ with $\xi_c(0)$ = 3.1 Å in YBCO layers [13]. This length is shorter than the distance between the CuO_2 planes $d(= 8.1$ Å) in two neighboring YBCO unit cells, as shown in the inset of Fig. 5. Thus, the Cooper pairs can hardly couple with each other along the c-axis direction and only pancake vortices exist to dominate the dissipation. On the other hand, ξ_c is around 11 Å at $t = 0.92$ so that it is longer than d. The Cooper pairs can couple with each other along the c axis in the YBCO layer and string vortices are formed and pinned at intrinsic weakly superconducting layers at higher temperature. Hence, at higher temperatures, both the pancake and the string vortices in the YBCO layers appear to cause the deviation of the dimensionality of flux dynamics from the 2D behavior.

In order to investigate the influence of the thickness of each YBCO layer on the dimensionality of flux dynamics at t = 0.92. The $J_c(\theta)$ curves for all samples under H = 0.1 T at $t = 0.92$ were measured and shown in Fig. 6. These data were fitted to a 2D scaling

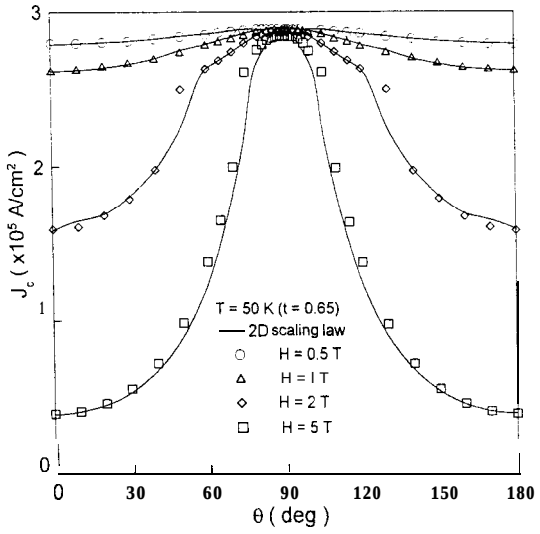


FIG. 4. Critical current demsities Jc as a function of angle θ for sample A under various H up to 5 T at t = 0.65. The 2D scaling law is denoted by the solid lines.

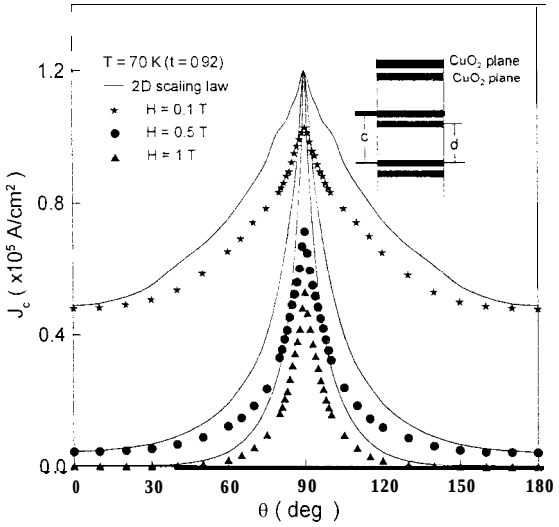


FIG. 5. Critical current densities J_c versus angle θ for sample A under various H up to 1 T at t = 0.92. The 2D scaling law is represented by the solid lines.

law represented by the solid lines. It was found that the $J_c(\theta)$ curves become closer to the 2D scaling law gradually as the thickness of each YBCO layer is increased from 48 Å (sample A) to 60 Å (sample B). For sample C with each YBCO layer 120 A-thick, the $J_c(\theta)$ curve can be fitted to the scaling very well. These results seem to imply that the dimensionality of flux dynamics tends to the 2D regine as the thickness of each YBCO layer is increased. However, the $J_c(\theta)$ curve for the 960 A-thick pure YBCO thin film (sample D) deviates from the 2D scaling law again.

The changes in the dimensionality of flux dynamics from sample A to C may be explianed by the following reason. At the higher temperature, both pancake vortices and string vortices exist and dominate the energy dissipation for sample A. This sample exhibits less anisotropy. When the thickness of each YBCO layer is increased, then the coupling among the Cooper pairs along the c axis becomes stronger. Meanwhile, the coupling along the ab plane also becomes stronger. At the same time, the increase in the coupling strength along the c axis is restricted because of the existence of the PYBCO layers. Hence, when the thickness of each YBCO layer is increased to 120 A, the coupling among Cooper pairs along the ab plane is stronger than that along the c axis. Thus, a superlattice with each thicker YBCO layer reveals more anisotropy and the pancake vortices then dominate the energy dissipation. By removing the PYBCO layers, as in the pure YBCO thin film, the restriction on the c-axis coupling vanishes and the couplings along the c axis and the ab plane become comparable. Hence, the dimensionality of flux dynamics turns to be closer to 3D for the pure YBCO thin film at $t = 0.92$.

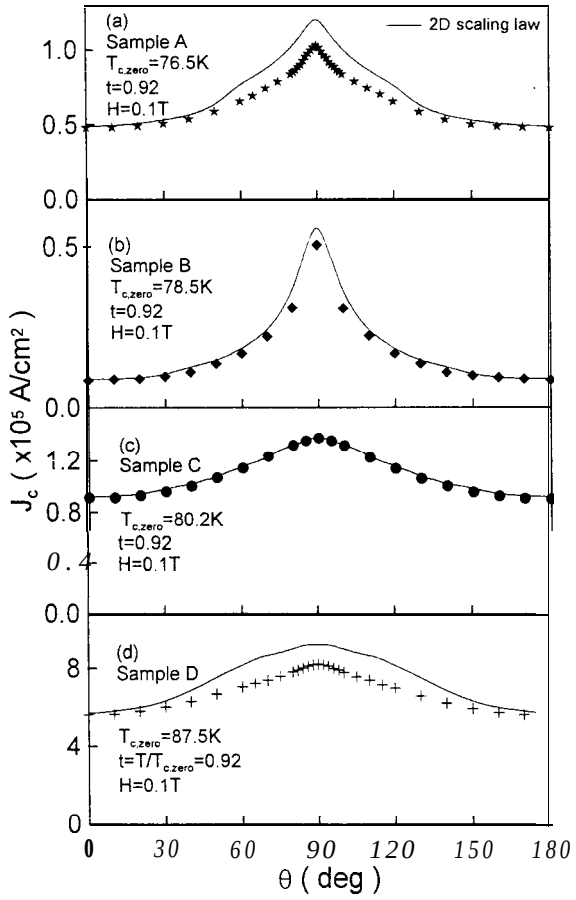


FIG. 6. Angular dependent critical current densities J,(B) for (a) sample A, (b) sample B, (c) sample C and (d) sample D under H = 0. 1 T at t = 0.92. These data are fitted to the 2D scaling law denoted by the solid lines.

It is notable that the energy dissipation is dominated by pancake vortices in sample C and that the contribution from the string vortices is negligible. Some experimental results indicate that the pinning potential decreases with increasing applied magnetic field [14]. Thus, if the ab-plane component of the applied magnetic field (H^{ab}) is increased while the c-axis component of the applied magnetic field (H^c) remains constant, then the string vortices should also contribute to the energy dissipation and the dimensionality of flux dynamics in sample C should deviate the 2D behavior. In order to verify this, a variety of magnetic fields $H^{ab}(= H\sin\theta)$ were applied with the same $H^c(= H\cos\theta =$ 0.1 T). The measured V-I curves for sample C at $t = 0.92$ are shown in Fig. 7. It was found that the V-I curves overlap under H^{ab} from zero field to 0.490 T and are shifted to the left as H^{ab} is increased to 0.995 T and 2.998 T. Voltages in the nonohmic region are due to the flux motion[15] and the overlap of V-I curves under low H^{ab} implies that the flux motion is not

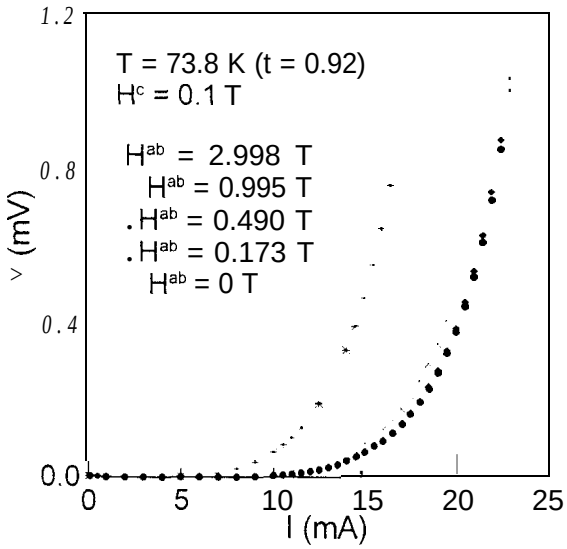


FIG. 7. V-I vurves for sample C at $t = 0.92$ and various H^{ab} with a fixed value of H^{c} (= 0.1 T).

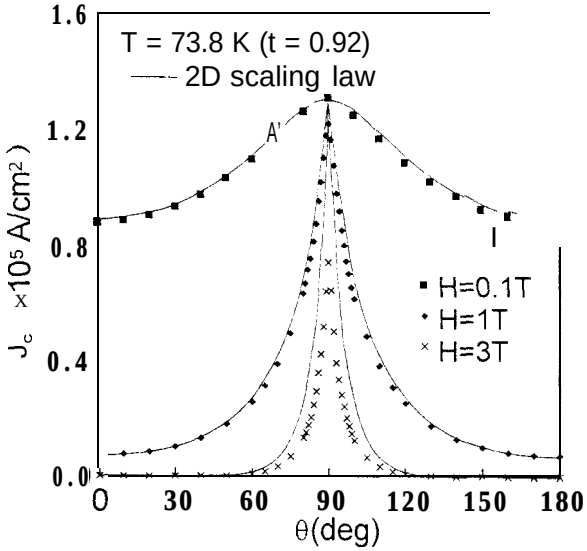


FIG. 8. J_c as a function of θ for sample C under applied magnertic fields of II = 0.1 T, 1 T and 3 T. The solid lines are the 2D scaling law.

influenced by H^{ab} but determined only by H". However, for higher H^{ab}, the shift in the V-I curves suggests that string vortices also participate in the energy dissipation. To investigate the influence of the applied magnetic field on the dimensionality of flux dynamics in sample C, the angular dependent critical current densities $J_c(\theta)$ under various applied magnetic fields at $t = 0.92$ were measured and shown in Fig. 8. It was found that the $J_c(\theta)$ curves can be fitted to a 2D scaling law very well under H = 0.1 T and 1 T. So that the flux dynamics for sample C shows a 2D behavior under $H < 1$ T at $t = 0.92$. For H = 3 T, $J_c(\theta)$ curve deviates from the scaling law at θ close to 90°, but follows it at θ around 0" and 180". This fact implies that the dimensionality of flux dynamics deviates from a 2D behavior under higher H^{ab}. By changing the ab-plane component of the applied magnetic field, the dimensionality of flux dynamics in YBCO/PYBCO superlattices can be 2D or close to 3D at high temperatures.

IV. Conclusions

Due to the temperature c-axis GL coherence length, the coupling strength between Cooper pairs along the *c* axis in the superconducting YBCO layers becomes stronger at higher temperatures and the dimensionality of flux dynamics in the YBCO/PYBCO (48Å/24Å)×20 superlattice is closer to be 3D. By increasing the thickness of each YBCO layer in the superlattice at higher temperatures, both the couplings along the *c* axis and the ab plane are enhanced. But due to the existence of the PYBCO layers, the coupling along the ab plane becomes stronger than that along the c axis if the thickness of the YBCO layer is 120 Å. Pancake vortices then dominate the energy dissipation and the contribution from

the string vortices is negligible. Their contribution grows as the ab-plane component of the applied magnetic field is increased. Thus, the dimensionality of flux dynamics deviate from a 2D behavior under larger applied magnetic field along the ab plane.

Acknowledgments

This work was supported by the National Science Council of R.O.C. under grant No. NSC86-2112-M003-012, NSC86-2112-M003-003, NSC86-2112-M002-033 and NSC86-2112-M002-013.

References

[1] M. Tachiki and S. Takahachi, Solid State Commun. 70, 291 (1989).
[2] M. Tachiki and S. Takahachi, Solid State Commun. 72, 1083 (1989).
[3] B. Roas, L. Schultz, and G. Saemann-Ischenko, Phys. Rev. Lett. 64, 479 (1990).
[4] G. Saemann-Ischenko *et al.*, International Seminor on High Temperature Superconductivity, Dutna, USSR, 28 June-l July 1989.
[5] P. H. Kes, J. Aarts, V. M. Vinokur, and C. J. van der Beek, Phys. Rev. Lett. 64, 1063 (1990).
[6] J. R. Clem, Phys. Rev. B43, 7837 (1991).
[7] H. H. Sung, J. T. Jeng, J. M. Wu, S. Y. Yang, H. E. Horng, L. M. Wang, and H. C. Yang, Chin. J. Phys. 34, 493 (1996).
[8] Q. Li, C. Kwon, X. X. Xi, Bhattacharya, A. Walkenhorst, T. Venkatsan, S. J. Hagen, W. Jiang, and R. L. Greene, Phys. Rev. Lett. 69, 2713 (1992).
[9] G. Jacob, M. Schmitt, Th. Kluge, C. Tome-Rosa, P. Wagner, Th. Hahn, and H. Adrian, Phys. Rev. **B47**, 12099 (1993).
[10] H. E. Horng, S. Y. Yang, J. T. Jeng, J. M. Wu, and H. C. Yang, IEEE Trans. Appl. Supercond. 7, 1177 (1997).
[11] S. Y. Yang, H. E. Horng, and H. C. Yang, Physica C 282-287, 1997 (1997).
[12] S. Y. Yang, J. T. Jeng, H. E. Horng, and H. C. Yang, Applied Superconductivity 1997: Proceedings of EUCAS 1997, pp. 157 (Institute of Physics Publishing, Bristol and Philadelphia, 1998).
[13] P. G. de Gennes, *Superconductivity of Metals and Alloys* (Addison-Wesley, New York, 1994).
[14] 0. Brunner, L. Antognazza, J. M. Triscone, L. Mieville, and Ø. Fisher, Phys. Rev. Lett. 67, 1354 (1991).
[15] M. Cryot and D. Pavuna, *Introduction to Superconductivity and High-T, Materials* (World Scientific, Singapore, 1992).